

Oleate Salt Formation and Mesomorphic Behavior in the Propranolol/Oleic Acid Binary System

KIERAN J. CROWLEY,[†] ROBERT T. FORBES,^{*†} PETER YORK,[†] HAKAN NYQVIST,[‡] AND OLA CAMBER[‡]

Contribution from *Drug Delivery Group, Postgraduate Studies in Pharmaceutical Technology, The School of Pharmacy, University of Bradford, Bradford, BD7 1DP, U.K., and Analytical and Pharmaceutical R&D, Astra Arcus, Södertälje, S-151 85, Sweden.*

Received December 28, 1998. Accepted for publication February 23, 1999.

Abstract □ Thermal analysis of propranolol/oleic acid mixtures prepared by solvent evaporation enabled construction of the binary system phase diagram. This allowed both physical and chemical interactions to be identified, including complex formation at the equimolar composition. An incongruent melting complex with a characteristic reaction point was identified in excess oleic acid compositions, a common property of fatty acid/fatty acid salt binary systems. The equimolar complex was confirmed to be propranolol oleate using infrared spectroscopy. Wide-angle X-ray powder diffractometry demonstrated that propranolol oleate possessed long-range positional order (~25 Å *d* spacing) accompanied by a degree of disorder over shorter *d* spacings. Such a pattern suggested mesophase formation, explaining the unctuous nature of propranolol oleate at room temperature. Accurate measurement of the long-range *d* spacing was achieved using small-angle X-ray scattering, permitting differentiation of the three different phases identified (phase I: 25.4 Å, phase II: 24.6 Å, phase III: 25.4–25.5 Å). The implications of drug fatty acid salt formation and also mesomorphism in pharmaceutical systems are discussed.

Introduction

The numerous gastrointestinal physiological effects of lipids can be utilized to manipulate drug oral bioavailability. Examples include extension of the gastrointestinal transit time, modified drug absorption, and stimulation of lymphatic drug transport.¹ Owing to the regional nature of these effects, drug and lipid must be released in a localized and controlled manner. During the initial development stages of such an oral drug delivery system, one must establish the physicochemical properties of drug, lipid, and the drug/lipid combination so that an appropriate system is chosen.

Oleic acid is a long chain fatty acid of considerable interest in oral drug delivery, as it has been shown to participate in all of the aforementioned physiological effects.^{2–4} An example of oral bioavailability enhancement following coadministration of oleic acid has been reported for the β -adrenoceptor blocking drug, propranolol.⁵ Administration of a propranolol/oleic acid binary mixture with a propranolol/oleic acid/polymer sustained release ternary mixture led to 3-fold bioavailability enhancement in humans. Propranolol human oral bioavailability is approximately 30% due to extensive first pass metabolism.⁶ In light of this, the effect of oleic acid is particularly significant because a postabsorption event appeared to be responsible.

Stimulation of propranolol lymphatic transport was considered but a cannulated lymphatic animal model failed to identify sufficient lymphatic drug transport that could impact on drug first pass metabolism.⁷ We have undertaken a physicochemical investigation of the propranolol/oleic acid binary system to identify alternative mechanisms of improved bioavailability caused by oleic acid coadministration.

Little is known about the solid-state physical and chemical properties of drug/fatty acid binary systems. The linear structure and polar properties of lipid molecules predispose them to mesophase formation.⁸ The term mesophase defines all levels of molecular order that are intermediate of the fully ordered crystalline state and the liquid or amorphous state. Subcategories are present within this broad definition, an example of which is provided by high purity oleic acid. At -6°C the fully ordered crystalline phase (γ) converts to a conformationally disordered crystalline mesophase (α), followed by melting to a neat phase at 13°C .⁹ The α -phase of oleic acid contains long range positional order in three-dimensions, but orientational disorder of the fatty acid chains is present within the lattice. Structures with a lower degree of positional order, in only one or two-dimensions, are classed as liquid crystalline.¹⁰

The aim of this study was to investigate the phase behavior of the propranolol/oleic acid binary system using thermal analysis, infrared spectroscopy, and X-ray crystallography. Construction of the binary system phase diagram allowed physical and chemical interactions to be identified. The analytical and pharmaceutical implications of complex formation and mesomorphism in the propranolol/oleic acid system are discussed.

Materials and Methods

Materials—Propranolol base was prepared by addition of excess sodium hydroxide to an aqueous solution of propranolol HCl (Sigma, Poole, U.K.), followed by extraction into chloroform and solvent evaporation. Thermal analysis of six batches found the propranolol base extrapolated onset of melting temperature ($91.6 \pm 0.6^\circ\text{C}$) and melting enthalpy ($148.4 \pm 1.8 \text{ J/g}$) to be in good agreement with literature values (92.9°C , 146.4 J/g).¹¹ Thermogravimetric analysis demonstrated 0.6% w/w (± 0.1 , $n=3$) weight loss during heating at 10°C/min from 25 to 150°C , and water content was found to be less than 0.1% w/w ($n=3$) using Karl Fischer titration. Binary mixtures of propranolol base and high purity oleic acid ($>99\%$, Sigma, Poole, U.K.) ranging from 5 to 95% P (% P: molar percentage of propranolol base) were prepared by evaporation from chloroform under 900 mbar vacuum at 25°C for 24 h to yield approximately 1 g product. Drug and fatty acid chemical structures are shown in Figure 1.

Methods—*Thermal Analysis*—Differential scanning calorimetry (DSC) was carried out using the Perkin-Elmer DSC-7 (Beaconsfield, U.K.). Binary mixtures were accurately weighed in the range 5–7 mg into stainless steel pans, hermetically sealed, and then

* To whom correspondence should be addressed. Tel 44-1274-384653. Fax 44-1274-234769. E-mail r.t.forbes@bradford.ac.uk.

[†] University of Bradford.

[‡] Astra Arcus.

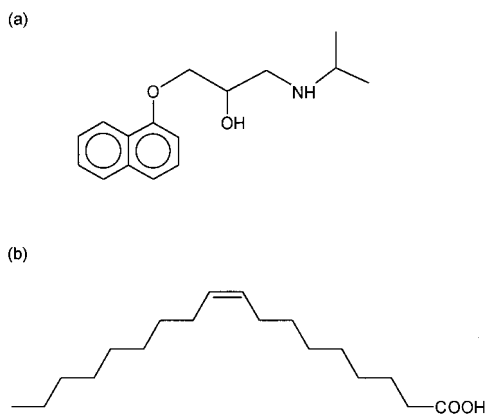


Figure 1—Chemical structures of (a) propranolol, (b) oleic acid.

stored at -17 to -15 °C for 18 h prior to analysis. Particle size control was not possible because many compositions were semisolid or liquid at room temperature. Cooled sample pans were rapidly transferred to the precooled DSC head and analyzed using varying heating rates from -30 to 110 °C. Temperature and enthalpy calibration was carried out using standard indium and zinc, with TAS-7 software for data analysis. All thermal event temperature values were the extrapolated onset temperature with the exception of the liquidus temperature calculation. This temperature represents the liquidus line of the phase diagram, the point above which a system is liquid. Peak melting temperature is therefore a more appropriate measure of the often broad liquidus endotherm and is used in this study.¹² DSC analyses were complemented with hot stage microscopy (HSM, Stanton Redcroft, London, U.K.) to confirm the nature of phase changes taking place.

Fourier Transform Infrared (FT-IR) Spectroscopy—FT-IR spectroscopy was carried out using a 6020 Galaxy spectrometer (Mattson, Newport Pagnell, U.K.) converting 250 scans over 4000 to 400 cm^{-1} at 4 cm^{-1} resolution to conventional frequency domain spectra. An attenuated total reflectance crystal (ATR crystal, Graseby-Specac, Orpington, U.K.) was used to allow analysis of solid, semisolid, and liquid samples. Samples were spread directly onto the crystal surface from chloroform solution and then analyzed at room temperature following solvent evaporation.

X-ray Crystallography—Wide-angle crystallographic data was obtained using a Siemens D5000 X-ray powder diffractometer (XRPD, Karlsruhe, Germany) with a $\text{Cu K}\alpha$ radiation source at generator settings of 40 kV and 30 mA. XRPD diffractograms were obtained at 22 °C over 1 – $30^\circ 2\theta$ (2θ , the angle between incident and reflected X-rays) using a step size of $0.01^\circ 2\theta$ and a count time of 1 s. Small-angle X-ray scattering (SAXS) was also completed using the Kratky Compact Camera (M. Braun Graz Optical Systems, Graz, Austria). Samples approximately 1 mm thick were mounted in a transmission sample holder between mica windows and cooled below -15 °C for 18 h. The sample stage was cooled to 4 °C with an Anton Paar Peltier temperature control device before sample transfer to stage. The camera tube was evacuated to 0.1 mbar and data collected for 10 min, using $\text{Cu K}\alpha$ radiation generated by the Philips 1830/40 generator at 40 – 45 kV and 35 – 40 mA. Measurements were made following 10 min isothermal holds to ensure sample temperature equilibration. Temperature control was accurate to ± 1 °C in the range 0 to 70 °C, with d spacings calibrated at 37 °C to 0.1 Å with tristearin.

Results

Thermal Analysis—Precooled propranolol/oleic acid binary mixtures prepared by solvent evaporation were analyzed using DSC. Representative DSC scans are shown in Figures 2a (excess propranolol) and Figure 3a (excess oleic acid). These data were used to construct the binary phase diagram, also presented in two parts (Figures 2b and 3b).

Binary mixtures containing excess propranolol were analyzed at 10 °C/min (Figure 2a). A new thermal event at 51 °C was present in all compositions increasing in

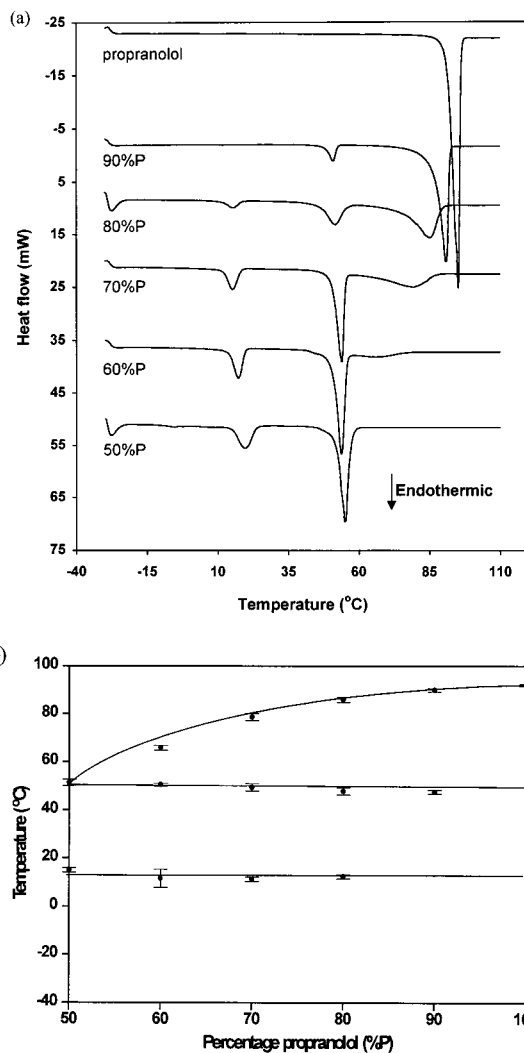


Figure 2—(a) DSC heating scans performed at 10 °C/min of propranolol/oleic acid binary mixtures containing excess propranolol (propranolol, 90% P, 80% P, 70% P, 60% P, 50% P). Compositions quoted as molar percentage % P. (b) Corresponding phase diagram. Three replicate DSC scans were used to obtain each phase transition temperature, the average of which is plotted with the standard deviation shown by an error bar.

magnitude as propranolol content decreased. The enthalpy of melting of excess propranolol decreased until absence at 50% P. The decreasing melting temperature of propranolol and also endotherm broadening suggested that solid propranolol was melting in a liquid phase. An initial melt at 51 °C followed by slow melting of excess propranolol was confirmed using HSM. Therefore, 51 °C corresponded to the solidus line of the phase diagram (the temperature below which the system was solid) and completion of excess propranolol melting represented the liquidus line. The 51 °C thermal event reached maximum enthalpy at 50% P, suggesting formation of an equimolar complex. The abbreviation POA is now used for this complex. The phase diagram indicated that propranolol had negligible solubility in molten POA immediately above the melting temperature of POA. Such a system is described as monotectic.¹² An endotherm at 13 °C also reached maximum enthalpy at POA, suggesting that POA underwent a phase change prior to melting at 51 °C. However, no macroscopic change could be observed when heating precooled POA using HSM.

Multiple thermal events in the second portion of the propranolol/oleic acid system were poorly resolved at 10 °C/min heating rate. Analysis at 2 °C/min provided improved thermal data presented in Figure 3a. The lower

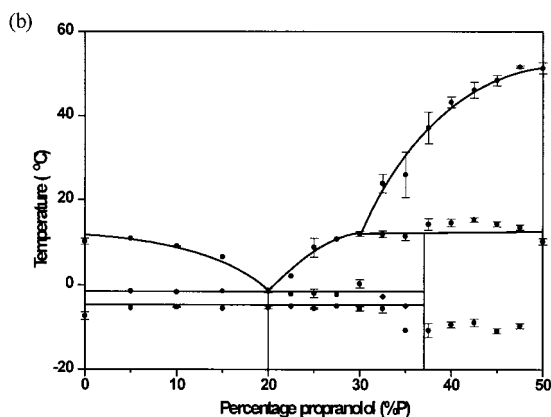
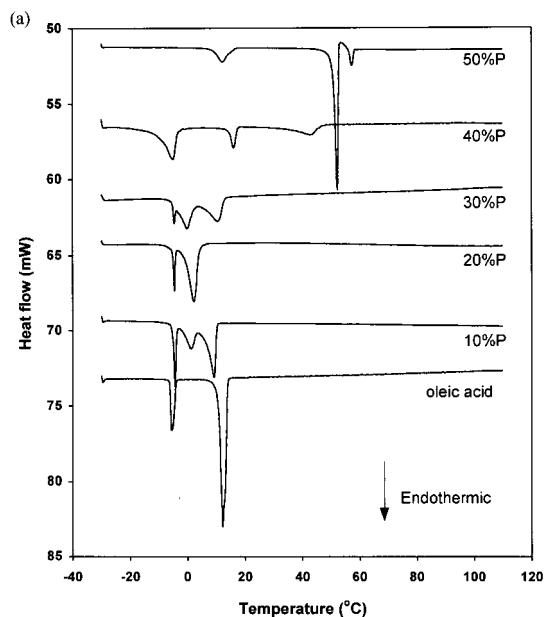


Figure 3—(a) DSC heating scans performed at 2 °C/min of propranolol/oleic acid binary mixtures containing excess oleic acid (50% P, 40% P, 30% P, 20% P, 10% P, oleic acid). Compositions quoted as molar percentage % P. (b) Corresponding phase diagram. For some compositions, three replicate DSC scans were used to obtain each phase transition temperature, the average of which is plotted with the standard deviation shown by an error bar.

heating rate produced a double endotherm at the POA melting event which is investigated in a following section. Eutectic system formation in excess oleic acid compositions was demonstrated by a depression in the liquidus line to a minimum of -1°C , accompanied by eutectic melting at -1°C in all 5–30% P compositions. The eutectic melt enthalpy was greatest at 20% P, the eutectic composition. The presence of the γ - α oleic acid phase transition at -6°C in 5–30% P compositions confirmed eutectic system formation because an eutectic is a two-phase system in the solid state. This explains why the γ - α transition was present in compositions when the α -oleic acid melting endotherm was absent.

The absence of the eutectic melt in mixtures 35–47.5% P, plus the discontinuity in the liquidus arm of the phase diagram at approximately 30% P, indicated formation of a second complex. The complex did not undergo congruent melting (where both solid and liquid phase have the same chemical composition). When a complex is stable as a solid but is not stable as a liquid phase of the same composition, the process is described as an incongruent melt.¹³ Such a melting process yields both a liquid and solid phase. This was apparent in the phase diagram (Figure 3b), and confirmation was obtained from the DSC curve for the

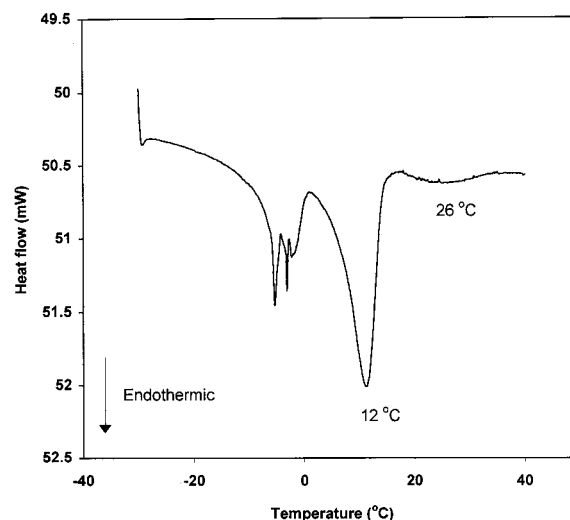
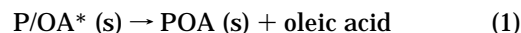


Figure 4—DSC heating scan performed at 2 °C/min of the 32.5% P binary mixture.

32.5% P composition shown in Figure 4. A complicated endothermic process between -6 and 0°C indicated the presence of the eutectic melt and oleic acid polymorphism. According to the simple eutectic phase diagram,¹² an eutectic melt is followed by a single liquidus endotherm that represents the melt of the excess component. However, a second low enthalpy melting endotherm (peak temperature, 26°C) could also be identified following the “liquidus” endotherm (peak temperature, 12°C). The endotherm at 26°C must be a product of the excess component melting event, confirming incongruent melting. The incongruent melting process of this complex, abbreviated as P/OA*, was as follows:



The composition of the incongruent melting complex was approximately 35–37.5% P, as indicated on the phase diagram. The break in the liquidus curve at approximately 30% P, 12°C , represented a reaction point and not the complex composition. Incongruent melting could not be identified using HSM because formation of a solid product during a melt cannot be distinguished from the final stages of a broad congruent melt. It was not possible to characterize the thermal event at approximately -10°C due to inadequate low temperature equilibration. Incongruent melting processes are commonly identified in fatty acid/fatty acid salt systems, suggesting that the equimolar complex POA was propranolol oleate.¹⁴

Fourier Transform Infrared (FT-IR) Spectroscopy—The physical properties of propranolol/oleic acid binary mixtures varied widely with composition as indicated on the phase diagram, and so an ATR crystal was used for spectroscopic investigation at room temperature. Spectra obtained for propranolol, oleic acid, and POA are displayed in Figure 5. The high-intensity absorption band at 1710 cm^{-1} of oleic acid was due to asymmetric stretch of the C=O group present in the stabilized fatty acid dimer. O–H out of plane bending of the carboxyl dimer was also identified by an absorption peak at 910 cm^{-1} . Both peaks were absent in POA. The propranolol absorption band at 3270 cm^{-1} due to N–H stretch of the free base was also absent in POA. A new absorption band was present in POA at 1552 cm^{-1} . This suggested formation of a stabilized carboxylate anion (corresponding to asymmetric stretch of COO^-) as seen in propranolol laurate¹⁵ and sodium oleate spectra.¹⁶ FT-IR confirmed that the equimolar complex POA was propranolol oleate.

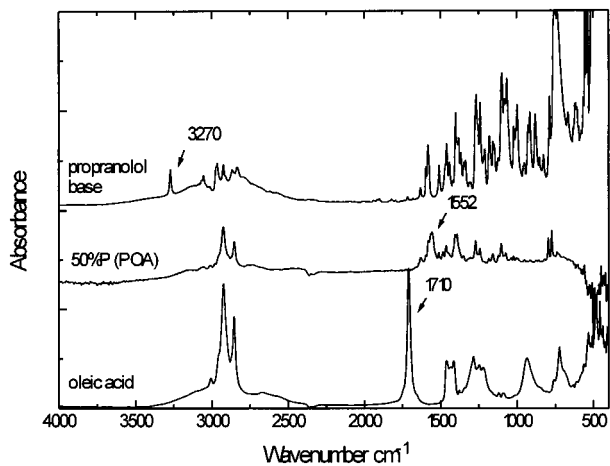


Figure 5—ATR FT-IR spectra of propranolol, 50% P (POA), and oleic acid at room temperature. The absence of secondary amine and carbonyl stretch bands at 3270 and 1710 cm^{-1} , respectively, and the presence of a new band at 1552 cm^{-1} (carboxylate anion) indicated salt formation.

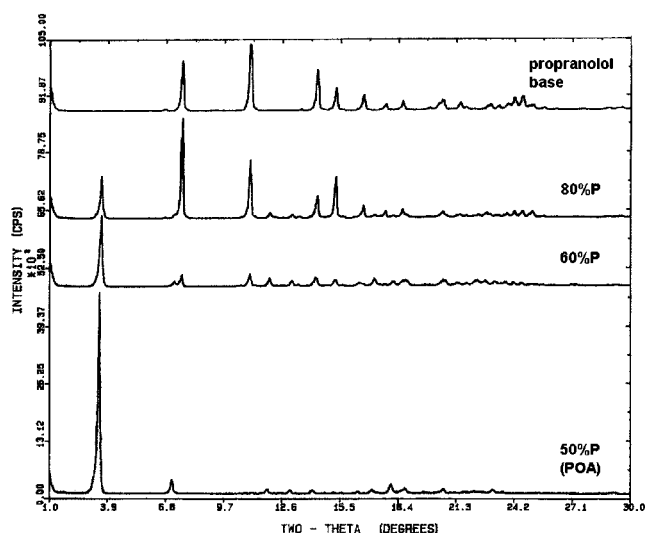


Figure 6—Wide-angle X-ray powder diffractometry (XRPD) patterns of propranolol, and binary mixtures 80% P, 60% P, and 50% P (POA) obtained over $1\text{--}30^\circ 2\theta$ at 22°C .

Wide-Angle X-ray Powder Diffraction (XRPD)—POA existed as an unctuous waxlike solid at room temperature with pronounced birefringence when viewed under crossed polarized light, suggesting mesomorphism. Many phase changes in excess oleic acid compositions took place beneath 22°C and could not be measured. XRPD diffractograms of 50, 60, 80% P and propranolol base were measured at 22°C (Figure 6). As the quantity of excess propranolol decreased, the intensity of propranolol reflections reduced until absence at the equimolar composition. Increasing POA content was marked by a high-intensity reflection at $3.7^\circ 2\theta$. The presence of both propranolol base and POA reflections at intermediate compositions indicated immiscibility of the two components in the solid state. This confirmed a two-phase monotectic system, as shown on the phase diagram (Figure 2b). The absence of high-intensity reflections in the $10\text{--}30^\circ 2\theta$ region of the POA spectrum indicated that this composition did not possess a rigid three-dimensional molecular lattice. Conversely, the absence of a broad “amorphous halo” in this region ruled out extensive molecular disorder. The high-intensity reflection at low angle demonstrated long-range positional order, approximate d spacing 24 \AA . New reflections of much reduced intensity were present at 7.3 and $11.0^\circ 2\theta$, corre-

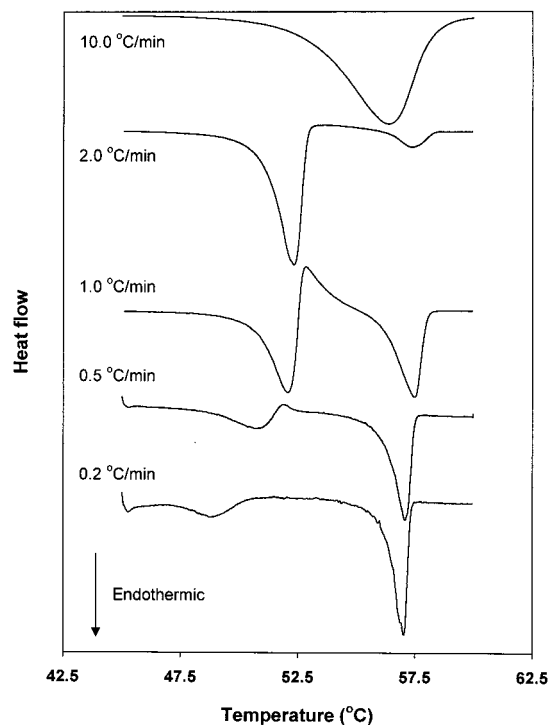


Figure 7—DSC heating scans of 50% P (POA) using variable heating rates (0.2, 0.5, 1.0, 2.0, and $10.0^\circ\text{C}/\text{min}$). Reduced heating rate reduces the magnitude of thermal events so the heat flow scale is averaged to facilitate data interpretation.

sponding to d spacings of 12.1 and 8.1 \AA . These appeared to be higher order reflections originating from the $\sim 24\text{ \AA}$ repeat unit. The relationship between the primary reflection ($\sim 24\text{ \AA}$ when $n = 1$) and higher order reflections (when $n = 2, 3, 4$, etc., from Bragg’s Law $n\lambda = 2d \sin \theta$) can be used to identify mesophase structure. The $\sim 24:12.1:8.1\text{ \AA}$ ($1:1/2:1/3$) ratio of different order reflections for POA indicated a layered structure, such as lamellar or smectic.¹⁷

Variable DSC Heating Rate Effect on POA Melting—Thermal analysis of precooled POA demonstrated an endothermic transition at 13°C . The low-temperature POA solid phase was termed form I, and the phase present above 13°C form II. A double endotherm at the POA form II melting temperature was observed when a DSC heating rate of $2^\circ\text{C}/\text{min}$ was used (Figure 3a). Further heating rate reduction led to identification of a third POA solid phase (III) that resolidified following form II melting (Figure 7). As heating rate was reduced, the magnitude of the higher temperature endotherm increased, because greater time was available for form III resolidification in a narrow temperature range. An isothermal period preceding form II melting resulted in complete resolidification of form III. This permitted accurate measurement of melting temperature and enthalpy for this form in the absence of concurrent exothermic processes. At the lowest heating rate of $0.2^\circ\text{C}/\text{min}$, the endothermic signal for form II melting was virtually absent due to simultaneous resolidification within the sample pan. HSM measurements were used to confirm simultaneous thermal events.

Small-Angle X-ray Scattering (SAXS)—In the absence of unique “fingerprint” XRPD patterns for POA forms I, II, and III, comprehensive thermal analysis provided the optimum tool for oleate salt mesophase characterization. Subtle changes in long-range positional order are commonplace during lipid phase changes (e.g., $\gamma\text{--}\alpha$ oleic acid phase transition).¹⁸ SAXS analysis of POA I showed two signals corresponding to 25.4 and 12.7 \AA (Figure 8a). The absence of high-intensity reflections at larger d spacings

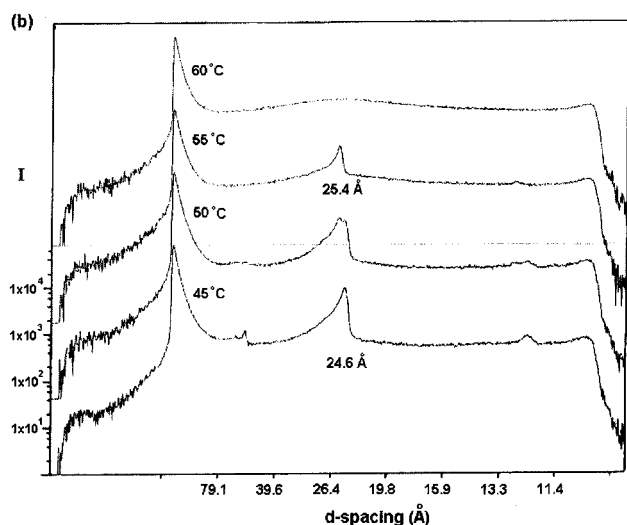
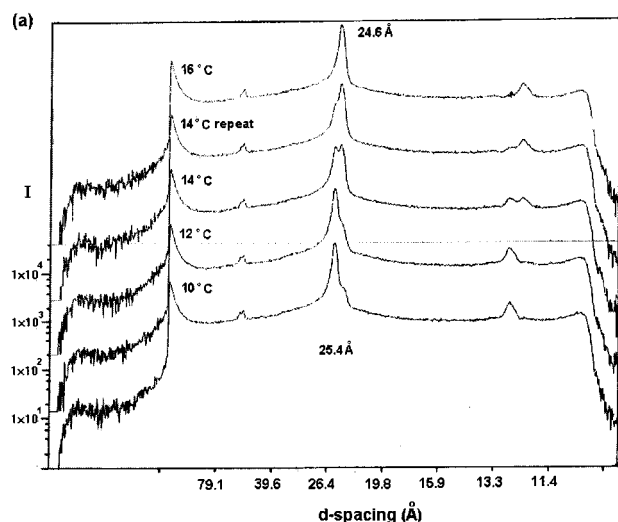


Figure 8—(a) Small-angle X-ray scattering (SAXS) patterns of pre-cooled 50% P (POA) heated from 10 to 16 °C at 2 °C increments. (b) 50% P (POA) heated from 45 to 60 °C at 5 °C increments. For both plots, data collection time was 10 min with a 10 min interval between measurements to allow temperature equilibration.

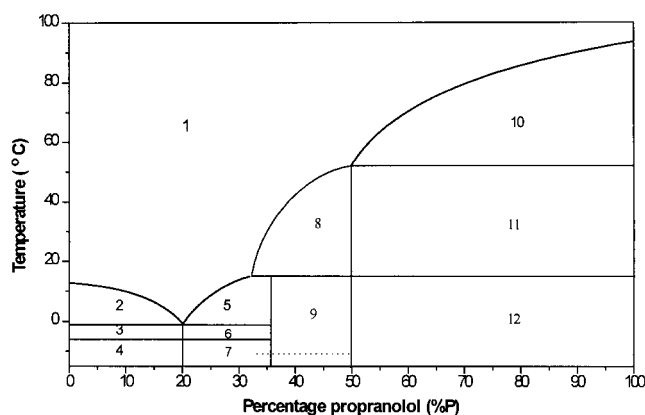


Figure 9—Propranolol/oleic acid binary system phase diagram. (1) miscible liquid phase, (2) α -oleic acid (s) and liquid, (3) α -oleic acid (s) and eutectic (s), (4) γ -oleic acid (s) and eutectic (s), (5) incongruent melting complex P/OA* (s) and liquid, (6) P/OA* (s) and eutectic containing α -oleic acid (s), (7) P/OA* (s) and eutectic containing γ -oleic acid (s), (8) equimolar complex POA II (s) and liquid, (9) P/OA* (s) and POA I (s), (10) propranolol (s) and liquid, (11) propranolol (s) and POA II (s), (12) propranolol (s) and POA I (s).

confirmed that the 25.4 and 12.7 Å signals represented the primary and secondary reflections. A decrease in the long-

Table 1—Summary of Propranolol Oleate Forms I, II, and III DSC (heating rate, 10 °C/min) and SAXS Data

form	temperature of melting/transition, °C (sd, $n = 6$)	enthalpy of transition, °C (sd, $n = 6$)	long-range d spacing, Å ($n = 3$)
I	13.1 (1.3)	23.9 (1.4)	25.4, 25.4, 25.4
II	51.4 (1.3)	77.3 (1.7)	24.6, 24.6, 24.6
III	55.7 (0.2)	58.7 (1.0)	25.5, 25.4, 25.5

range repeating unit took place on I–II conversion, as indicated by a fall in reflections to 24.5 and 12.3 Å. A small but significant structural change was also identified following gradual heating through POA II melting point to enable form III resolidification (Figure 8b). The repeating unit in POA III was found to be 25.4/25.5 Å. Thermal and crystallographic properties of POA forms I, II, and III are summarized in Table 1.

Discussion

The propranolol/oleic acid binary phase diagram contained important information concerning physical interactions such as monotectic and eutectic systems and also chemical interactions (complex formation). The presence of an incongruent melting complex and reaction point is commonly reported in fatty acid/fatty acid salt binary mixtures.¹⁴ In such systems “acid soap” complexes commonly form that undergo peritectic transformation at the reaction point. The peritectic transformation also marked by a reaction point, but the stable low-temperature solid phase is a solid solution.¹⁹ The transformation temperature often corresponds to a thermotropic polymorphic change of the fatty acid salt, as was seen in the oleic acid/propranolol oleate (POA) portion of the phase diagram (Figure 3b). Solid solution formation was not identified in this system. However, the presence of multiple thermal events at many compositions obstructed accurate measurement of transition enthalpies which are required for such calculations, and so solid solution formation cannot be ruled out. The presence of incongruent melting in phase equilibria is significant because it leads to extremely slow equilibration on cooling. Such behavior is of great importance in the fields of ceramics and metallurgy, but is rarely reported in the pharmaceutical sciences with the following exceptions.^{20–22} Incongruent melting complex formation in the propranolol/oleic acid system was thought to have contributed to the slow equilibration of binary mixtures in this region.

Incongruent melting can only be identified by interpretation of the phase diagram. DSC or HSM analysis of a single composition would consist of the incongruent melt followed by solid product melting, which would be interpreted as a two-phase solid sample undergoing separate melting processes. This melt is a single-step process, and so further decrease in heating rate will not alter the relative enthalpies of incongruent melt to solid product melt. However, the effect of heating rate was evident during DSC analysis of two simultaneous thermal events. A change in heating rate altered the relative magnitude of two simultaneous processes, causing marked changes in the DSC total heat flow signal (Figure 7). The latter example demonstrated the importance of complementing DSC data with HSM analysis under similar conditions.

It is emphasized that the phase diagram presented does not represent the equilibrium phase diagram for this system. In addition to the fact that phase behavior beneath -10 °C was not investigated, the impact of POA III formation was omitted. POA II was the most stable form

at room temperature, as shown by DSC analysis of 50–90% P compositions following 6 and 12 months. Therefore, the phase diagram presented was of practical relevance. XRPD indicated that POA II exhibited mesomorphic properties as seen by the presence of long range order accompanied by considerable molecular disorder over shorter distances. The fact that this phase underwent a high enthalpy melt, and that resolidification took place post-melting, strongly suggested that POA II was a conformationally disordered crystalline phase. Liquid crystalline transitions are generally of a lower enthalpy than the initial breakdown of three-dimensional order (crystalline phase) and do not revert to higher ordered structures on temperature increase.¹⁰ XRPD data for POA III showed the absence of high intensity reflections at wide-angle, and so this phase was also classified as a conformationally disordered mesophase. XRPD data was not obtained for POA I so description of this phase is not possible. Nevertheless, SAXS enabled accurate measurement of the long-range repeating unit of all POA solid phases I, II, and III, for which small but significant differences were found.

Oral bioavailability improvement was reported following propranolol laurate administration,²³ and propranolol stearate modified drug entry into the systemic circulation following nasal administration.²⁴ Thus, the formation of propranolol oleate salt in the propranolol/oleic acid system is likely to have biopharmaceutical implications. In particular, oleate salt formation within the dosage form or in the gastrointestinal tract may have contributed to the increased bioavailability of a propranolol/oleic acid/polymer oral dosage form reported by Barnwell et al.⁵ The encouraging effects of propranolol and fatty acid coadministration mean that such drug/lipid systems warrant further investigation, but their complicated phase behavior must be fully understood to enable optimal formulation.

Conclusion

The propranolol/oleic acid binary system phase diagram was constructed using thermal analysis, and equimolar complex and incongruent melting complex formation was demonstrated. The equimolar complex, POA, was identified as propranolol oleate using FT-IR. At room temperature, POA possessed substantial long range positional order accompanied by disorder over shorter *d* spacings as shown by XRPD. This phase (POA II) was classified as a conformationally disordered crystalline phase. SAXS allowed accurate measurement of the long-range repeating unit, leading to the identification of subtle structural changes following POA I, II, and III conversions. Formation of an oleate salt provides an interesting approach for oleic acid inclusion in solid oral dosage forms, but the propensity for complicated phase behavior must be considered. Characterization of the propranolol/oleic acid binary system has demonstrated that a thorough understanding of drug/lipid interactions is vital when formulating such materials.

References and Notes

1. Charman, W. N.; Porter, C. J. H.; Mithani, S.; Dressman, J. B. Physicochemical and physiological mechanisms for the effects of food on drug absorption. *J. Pharm. Sci.* **1997**, *86*, 269–281.

2. Brown, N. J.; Read, N. W.; Richardson, A.; Rumsey, R. D. E.; Bogentoft, C. Characteristics of lipid substances activating the ileal brake in the rat. *Gut* **1990**, *31*, 1126–1129.
3. Muranishi, S. Modification of intestinal absorption of drugs by lipoidal adjuvants. *Pharm. Res.* **1985**, *2*, 108–118.
4. Charman, W. N.; Stella, V. J. Transport of lipophilic molecules by the intestinal lymphatic system. *Adv. Drug Del. Rev.* **1991**, *7*, 1–14.
5. Barnwell, S. G.; Burns, S. J.; Higginbottom, S.; Whelan, I.; Corness, D.; Hay, G.; Rosenberg, E.; Attwood, D. Demonstration of the importance of biphasic oleic acid delivery for enhancing the bioavailability of propranolol in healthy volunteers. *Int. J. Pharm.* **1996**, *128*, 145–154.
6. Riddell, J. G.; Harron, D. W. G.; Shanks, R. G. Clinical pharmacokinetics of β -adrenoceptor antagonists. *Clin. Pharmacokin.* **1987**, *12*, 305–320.
7. White, D. G.; Story, M. J.; Barnwell, S. G. An experimental animal model for studying the effects of a novel lymphatic drug delivery system for propranolol. *Int. J. Pharm.* **1991**, *69*, 169–174.
8. Small, D. M., Ed. *Handbook of Lipid Research 4. The Physical Chemistry of Lipids*; Plenum Press: New York, 1988.
9. Kobayashi, M.; Kaneko, F.; Sato, K.; Suzuki, M. Vibrational spectroscopic study on polymorphism and order-disorder phase transition in oleic acid. *J. Phys. Chem.* **1986**, *90*, 6371–6378.
10. Leadbetter, A. J. Structural classification of liquid crystals. In *Thermotropic Liquid Crystals*; Gray, G. W., Ed.; J. Wiley and Sons: U.K., 1987; pp 1–27.
11. Neau, S. H.; Shinwari, M. K.; Hellmuth, E. W. Melting point phase diagrams of free base and hydrochloride salts of bevantolol, pindolol and propranolol. *Int. J. Pharm.* **1993**, *99*, 303–310.
12. Ford, J. L.; Timmins, P. *Pharmaceutical Thermal Analysis: Techniques and Applications*; Ellis Horwood: Chichester, U.K., 1989.
13. Atkins, P. W., Ed. *Physical Chemistry*, 6th ed.; Oxford University Press: U.K., 1998.
14. Cheda, J. A. R.; Ortega, F.; Sanchez-Arenas, A.; Cosio, A.; Fernandez-Garcia, M.; Fernandez-Martin, F.; Roux, M. V.; Turrion, C. Binary phase diagrams of lead(II) *n*-alkanoates and *n*-alkanoic acids. *Pure Appl. Chem.* **1992**, *64*, 65–71.
15. Ogiso, T.; Shintani, M. Mechanism for the enhancement effect of fatty acids on the percutaneous absorption of propranolol. *J. Pharm. Sci.* **1990**, *79*, 1065–1071.
16. Crowley, K. J. Unpublished results.
17. Harwood, J. L.; Padley, F. B. X-ray diffraction. In *The Lipid Handbook*, 2nd ed.; Gunstone, F. D., Harwood, J. L., Padley, F. B., Eds.; Chapman and Hall: London, 1994; pp 538–539.
18. Suzuki, M.; Ogaki, T. Crystallization and transformation mechanisms of α -, β -, and γ -polymorphs of ultrapure oleic acid. *J. Am. Oil Chem. Soc.* **1985**, *62*, 1600–1604.
19. McKie, D.; McKie, C. *Crystalline Solids*; Nelson: Walton-on-Thames, U.K., 1980; pp 506–557.
20. El-Banna, H. M.; El-Gholmy, Z. A.; Hammouda, Y. Phase diagram and dissolution rate studies on hydrochlorothiazide-urea solid dispersions. *Pharm. Acta Helv.* **1980**, *55*, 244–248.
21. Grant, D. J. W.; Jacobson, H.; Fairbrother, J. E.; Patel, C. G. Phases in the paracetamol-phenazone system. *Int. J. Pharm.* **1980**, *5*, 109–116.
22. Winfield, A. J.; Al Saidan, S. M. H. Compound formation in phenobarbitone-urea systems. *Int. J. Pharm.* **1981**, *8*, 211–216.
23. Aungst, B. J.; Hussain, M. A. Sustained propranolol delivery and increased oral bioavailability in dogs given a propranolol laurate salt. *Pharm. Res.* **1992**, *9*, 1507–1509.
24. Hussain, A.; Hirai, S.; Bawarshi, R. Nasal absorption of propranolol from different dosage forms by rats and dogs. *J. Pharm. Sci.* **1980**, *69*, 1411–1413.

Acknowledgments

The support of the Analytical and Pharmaceutical Department at Astra Arcus AB, Sweden, is gratefully acknowledged for provision of a graduate research studentship for K.J.C., and for access to small-angle X-ray equipment.

JS9804967